Electronic Supplementary Material (ESI) for ChemComm.
This journal is © The Royal Society of Chemistry 2019

Supporting information for

Rational modulation of coumarin–hemicyanine platform based on OH substitution for higher selective detection of hypochlorite

Jin-Shuai Lan[a,b#], Li Liu[b#], Rui-Feng Zeng[b], Yan-Hong Qin[b], Yun Liu[a,b], Xiao-Yi Jiang[b], Ayinazhaer Aihemaiti[b], Yue Ding[a,b]*, Tong Zhang[a,b]*, Rodney J.Y. Ho[c]

[a] *Experiment Center of Teaching & Learning, Shanghai University of Traditional Chinese Medicine, Shanghai, China;*

[b] *School of Pharmacy, Shanghai University of Traditional Chinese Medicine, Shanghai, China;*

[c] *Department of Pharmaceutics, University of Washington, Seattle, WA, USA;*

*Correspondence: zhangtongshutcm@hotmail.com (T.Z.);

dingyue-2001@hotmail.com (Y.D.);

Tel.: +86-021-51322318 (T.Z.)

# These authors contributed equally to this work.

1. Experimental section

1.1 Instrumentation and chemicals

Unless otherwise stated, chemicals used in the experiment were purchased from Sinopharm Chemical Reagent (Shanghai, China) and used directly. Nuclear magnetic resonance (NMR) spectra were obtained from a spectrometer (Bruker AVANCE III, Bruker, Germany) at 400 MHz, and tetramethylsilane was used as a reference for chemical shifts. Mass spectrometric results were obtained using an LC/MSD Trap mass spectrometer (6460 Series, Agilent). All ultraviolet (UV) absorbance measurements were conducted using the UV–vis spectrometer (8454, Agilent technologies, USA). All fluorescence spectra experiments were performed using a fluorescence spectrophotometer (G9800A, Agilent). The fluorescent bioimages were obtained using a multiphoton confocal microscope (TCS-SP8, Leica Wetzlar, Germany) with an oil-immersion/dry objective lens and the IVIS Lumina XR Imaging System (PerkinElmer, America). Analytical reagents and deionized water produced from a barnstead (TANKPE030, Morey Biosciences, France) were used for preparing the solutions.

1.2 Synthesis of probes

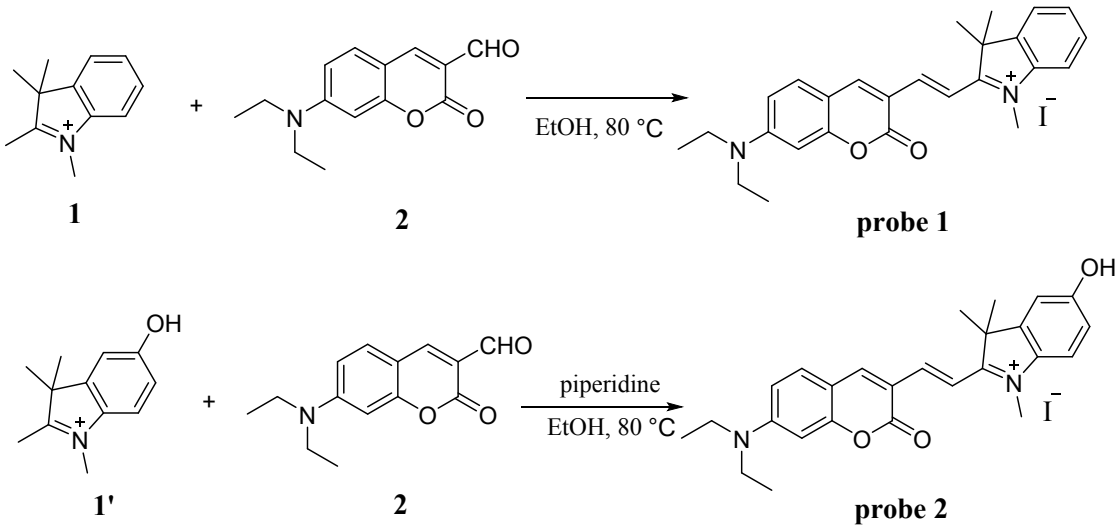

Scheme S1. Synthesis of probe **1** and probe **2.**

The synthetic route of probe **2** was shown in Scheme S1, and probe **1** can be synthesized according to the previous report.[S1] For probe **2**, under nitrogen, piperidine (30 μL) was added to a mixture of 5-Hydroxy-1,2,3,3-tetramethyl-3H-indol-1-ium iodide (**1'**) (50.00 mg, 0.158 mmol) and 7-(diethylamino)-3-formyl-coumarin (**2**) (38.67 mg，0.158 mmol) in dry EtOH (15 mL), then the reaction solution was stirred

at 80 °C and refluxed for 5 h. After cooling to room temperature, the reaction solution was concentrated in vacuo. The residual was dissolved with dichloromethane (DCM) and washed three times with water. The crude product was purified on silica-gel by column chromatography using DCM/MeOH (20:1 to 10:1, v/v) as eluent to afford probe **2** as a dark purple solid. ^{1}H NMR (400 MHz, DMSO-d_6) δ 10.29 (s, 1H), 10.29 (s, 1H), 8.75 (s, 1H), 8.09 (d, *J* = 15.9 Hz, 1H), 7.76 (d, *J* = 16.0 Hz, 1H), 7.66 (t, *J* = 10.2 Hz, 1H), 7.55 (d, *J* = 9.1 Hz, 1H), 7.15 (d, *J* = 2.3 Hz, 1H), 6.94 (dd, *J* = 8.7, 2.3 Hz, 1H), 6.88 (dd, *J* = 9.1, 2.3 Hz, 1H), 6.68 (d, *J* = 2.1 Hz, 1H), 5.74 (s, 1H), 3.92 (s, 3H), 3.61–3.46 (m, 4H), 1.70 (s, 6H), 1.16 (t, *J* = 7.0 Hz, 6H). ^{13}C NMR (100 MHz, DMSO-d_6) δ 178.37, 159.95, 159.41, 157.75, 153.94, 149.62, 147.00, 145.94, 134.49, 132.40, 116.27, 115.93, 112.90, 111.49, 111.17, 110.35, 109.58, 96.95, 51.63, 45.20, 34.26, 26.39, 12.94. MS: [M^+] at 417.21.

1.3 Sample preparation

The probes (1 mM) were dissolved by dimethyl sulfoxide (DMSO) to give a purple solution, which were diluted with PBS buffer solution (pH 7.4, 10 mM) for tested solutions (10 μM) at room temperature. Sodium hypochlorite aqueous solution (Chemical Pure, 5% available chlorine) and other anions (NO_2^-, HCO_3^-, Br^-, CO_3^{2-}, SO_4^{2-}, Ac^-, $H_2PO_4^-$, HPO_4^{2-}, Cl^-, S^{2-}, CN^-, I^-, H_2O_2, HSO_3^-, SO_3^{2-}) were purchased from Sinopharm Chemical Reagent Co., Ltd. (Shanghai, China). The remaining ionic solutions ($^1O_2$, H_2O_2, ·OH, NO, $ONOO^-$) are formulated by the literature.[S2] All those ionic solutions were prepared with purified water.

Due to the high sensitivity and rapid response of probe **2**, the concentration of ClO^- in the sample can be estimated easily, promptly and inexpensively. After reacting with water containing different concentrations of ClO^- (0, 5, 10, 20, 30, 40, 50, 60, 70，80，100，150，200 μM), the blue-violet of probe **2** faded as the amount of ClO^- increased. The result means that the probe **2** can be used to conveniently estimate the ClO^- content by colorimetry.

1.4 Cell culture and fluorescence imaging

HepG2 cells and RAW cells were cultured in Dulbecco's modified Eagle medium (DMEM) containing 10% fetal bovine serum and 1% Antibiotic-Antimycotic at 37 °C in the air incubator which contain 5% CO_2. They were together used to estimate the sensing capacity of probe **2** for endogenous and exogenous ClO^-.

For fluorescence imaging, HepG 2 cells (8×10^3/well) were cultured on confocal dishes and incubated for 24 h. Immediately before the staining experiment, cells were washed three times with PBS, and then incubated with probe **2** (10 μM) for 1 h at 37 °C. Then the petri dish was washing with PBS for another three times, then was incubating with different concentrations of ClO^- for 1 h at 37 °C. Observation and imaging were performed by Fluorescence Microscope and a 63×oil-immersion objective lens (Leica). The samples were excited at 405 nm (yellow channel) and 488 nm (red channel). Emissions were collected respectively at blue channel (480-520 nm) and red channel (630-680 nm).

RAW 264.7 macrophage cells were also sowed in confocal dishes with an equal cell density. After 24 h, the cells were incubated with the addition of 2 μg/mL LPS for 0, 12 or 24 h, respectively, then washed by PBS, and stained with probe **2** (10 μM) in culture media for 1 h at 37 °C. After washing the cells with PBS for three times, the bioimaging of RAW 264.7 cells were conducted by the same way that of HepG2 cells.

1.5. Zebra fish culture and imaging

Zebrafish embryos were maintained, incubated and developed in E3 embryo culture medium (containing 0.7 mM $NaHCO_3$, 0.5 mM KCl, 1 mM $MgSO_4$, 1 mM $CaCl_2$, 0.05 mM Na_2HPO_4, and 15 mM NaCl, 0.15 mM KH_2PO_4) at 28 °C. Newly hatched zebrafish were pretreated with ClO^- (0, 2, 5 μM) for 1 h, and residual ClO^- was then cleaned by deionized water, the zebrafish was further fostered with 10 μM probe **2** for another 1 h.

In order to estimate the sensitivity of probe **2** for endogenous hypochlorite in zebrafish, the zebrafish were pretreated with1 or 2 μg/mL LPS for 6 h, then washed by deionized water, and stained with 10 μM probe **2** configured by E3 embryo culture medium for 1 h under normal room temperature. For a control group, extra zebrafish

were fostered purely with probe **2** (10 μM) for 1 h and were washed by deionized water for three times before further bioluminescence observation. The fluorescence observation was conducted by an inverted confocal microscopy (Nikon A1MP) matched with a CCD camera, and the dry objective lens (10 ×) was applied. Besides, two excitation wavelengths were set at 405 and 488 nm respectively, and two emission wavelengths were collected at 480-520 nm and 630-680 nm respectively.

1.6. *In vivo* imaging of HOCl in a mouse model

Based on the Animal Management Rules of the Ministry of Health of China, all animal experiments were performed by guided on the Care and Use of Laboratory Animals of Shanghai University of Traditional Chinese Medicine. For λ-carrageenan-induced arthritis model, 100 μL of λ-carrageenan (5 mg/mL, in PBS) were injected into the right tibiotarsal joints (right ankles) of 8-10-week-old mice. The left tibiotarsal joints (injected the same volume of saline) generated a control group. Then the same amount of probe **2** (10 μL, 1 mM) were injected into both ankles with after 4 hours. For LPS-induced arthritis model, 100 μL LPS (5 mg/mL, in PBS) was injected into the right tibiotarsal joints (right ankles) of mice, and the left ankles were as a control. After 24 hours, the left and right ankles were injected with the same amount of probe **2** (10 μL, 1 mM). *In vivo* images were gained by using the VIS Lumina XR Imaging System (PerkinElmer, Massachusetts, America) with time.

2. Supporting Tables and Figures

Table S1. Comparison of the probes for the detection of ClO^-

Reference	Ratiometric Detection	$\lambda_{ex}/\lambda_{em}$ (nm)	Detection Limit (nM)	Time (s)	Bioimaging
[S3]	YES	420/478,420/610	25	13	RAW 264.7 cells
[S4]	NO	620/683	9.2	20	Hela cells
[S5]	NO	545/685	164	300	RAW 264.7 cells
[S6]	YES	540/587,540/619	59	30	Hela cells & zebrafish
[S7]	NO	365/435	5.89	135	HeLa cells & RAW 264.7 cells
[S8]	YES	475/495,475/618	4.6	5	RAW 264.7 cells & mice
[S9]	NO	480/525	62	100	HeLa cells & RAW 264.7 cells
[S10]	NO	310/472	0.16	10	HeLa cells
[S11]	NO	458/515	0.65	300	RAW 264.7 cells
This work	YES	420/500, 566/650	49.1	120	RAW 264.7 cells & HepG2 cells & zebrafish & mice

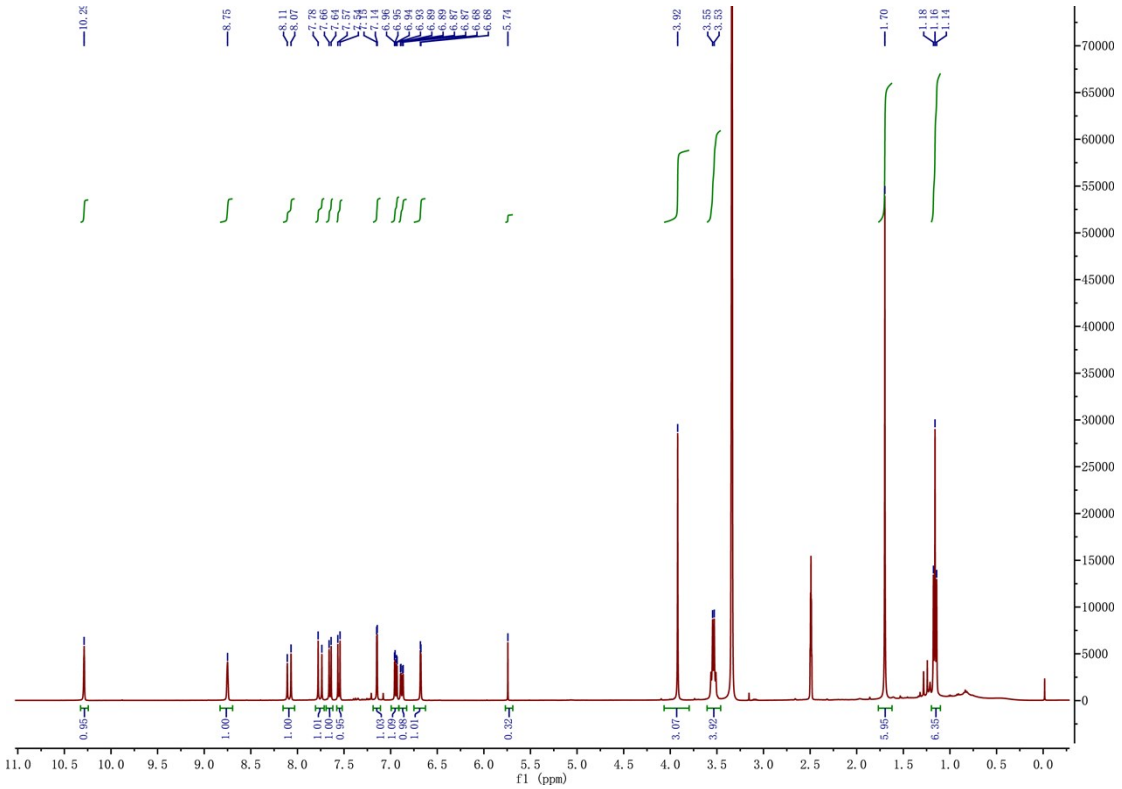

Fig. S1. ^{1}H-NMR spectra of the probe **2** in DMSO-d_6.

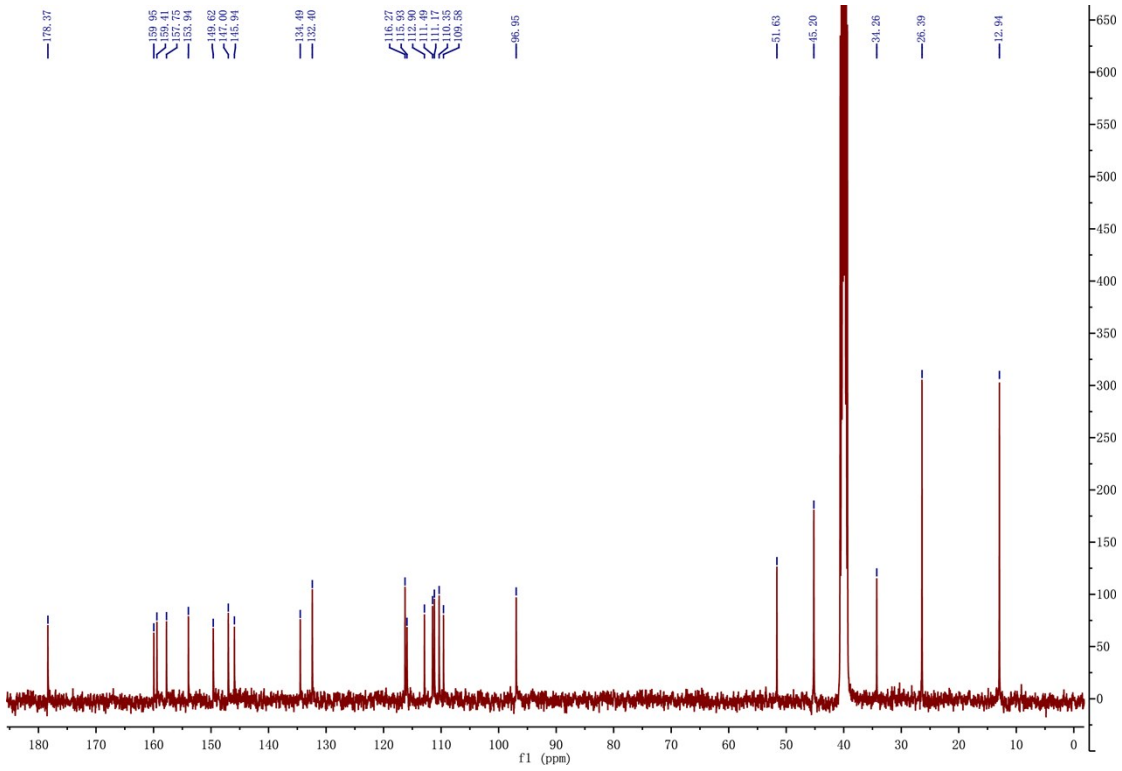

Fig. S2. ^{13}C-NMR spectra of the probe **2** in DMSO-d_6.

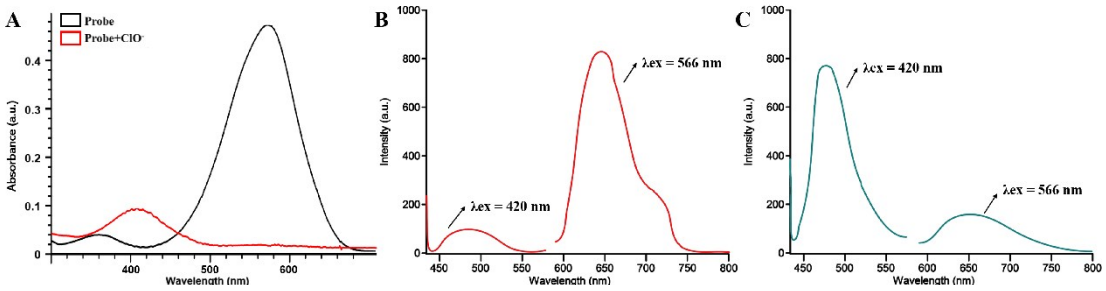

Fig. S3. (A) The UV-vis absorption spectra changes of probe **1** (10 μM) with ClO^- (100 μM) in PBS buffer solution (pH 7.4); (B) The fluorescence intensity of probe **1** (10 μM) in PBS buffer solution (pH 7.4); (C) The fluorescence intensity changes of probe **1** (10 μM) with ClO^- (100 μM) in PBS buffer solution (pH 7.4). λ_{ex} = 566 nm, slits: 5.0/5.0 nm at 650 nm; λ_{ex} = 420 nm, slits: 5.0/5.0 nm at 500 nm.

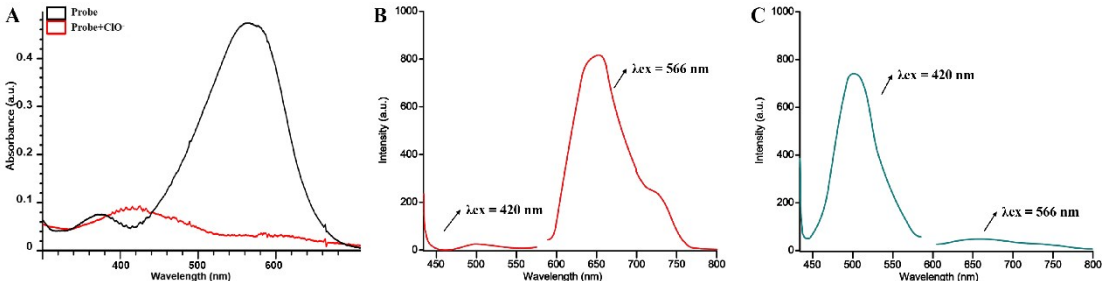

Fig. S4. (A) The UV-vis absorption spectra changes of probe **2** (10 μM) with ClO^- (100 μM) in PBS buffer solution (pH 7.4); (B) The fluorescence intensity of probe **2** (10 μM) in PBS buffer solution (pH 7.4); (C) The fluorescence intensity changes of probe **2** (10 μM) with ClO^- (100 μM) in PBS buffer solution (pH 7.4). λ_{ex} = 566 nm, slits: 5.0/5.0 nm at 650 nm; λ_{ex} = 420 nm, slits: 5.0/5.0 nm at 500 nm.

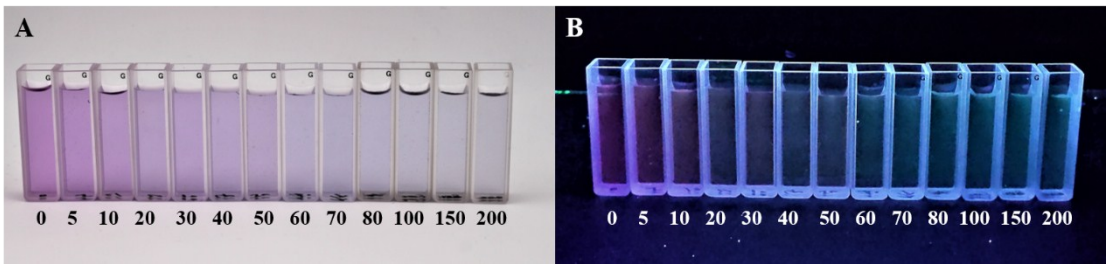

Fig. S5. (A) The color change of fluorescent probe **2** from bluish violet color to colorless with the increasing amount of ClO^- (0-200 μM) under sunlight; (B) The color change of fluorescent probe **2** from bluish violet color to glaucous with the increasing

amount of ClO^- (0-200 μM) under UV 365 nm.

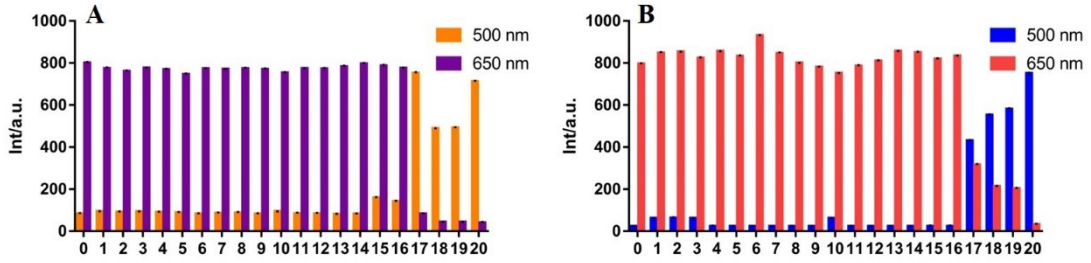

Fig. S6. (A) The fluorescence intensity of the probe **1** (10 μM) at 650 nm and 500 nm changes upon ClO^- and other anions (100 μM) in PBS buffer solution (pH 7.4); (B) The fluorescence intensity of the probe **2** (10 μM) at 650 nm and 500 nm changes upon ClO^- and other anions (100 μM) in PBS buffer solution (pH 7.4). (0) Black, (1) NO_2^-, (2) HCO_3^-, (3) Br^-, (4) CO_3^{2-}, (5) SO_4^{2-}, (6) Ac^-, (7) $H_2PO_4^-$, (8) HPO_4^{2-}, (9) Cl^-, (10) S^{2-}, (11) CN^-, (12) I^-, (13) $^1O_2$, (14) H_2O_2, (15) ·OH, (16) NO, (17) $ONOO^-$, (18) HSO_3^-, (19) SO_3^{2-}, (20) ClO^-. λ_{ex} = 566 nm, slits: 5.0/5.0 nm at 650 nm; λ_{ex} = 420 nm, slits: 5.0/5.0 nm at 500 nm.

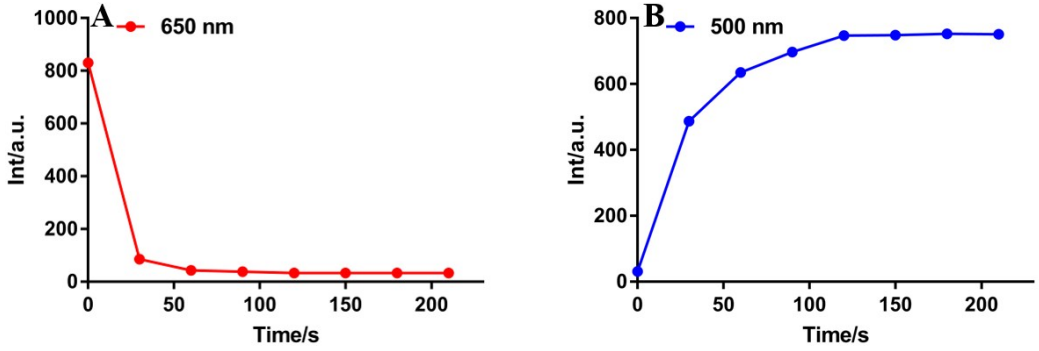

Fig. S7. Time-dependent fluorescent emission of probe **2** (10 μM) within ClO^- (100 μM) at 650 nm (A) and 500 nm (B). λ_{ex} = 566 nm, slits: 5.0/5.0 nm at 650 nm; λ_{ex} = 420 nm, slits: 5.0/5.0 nm at 500 nm.

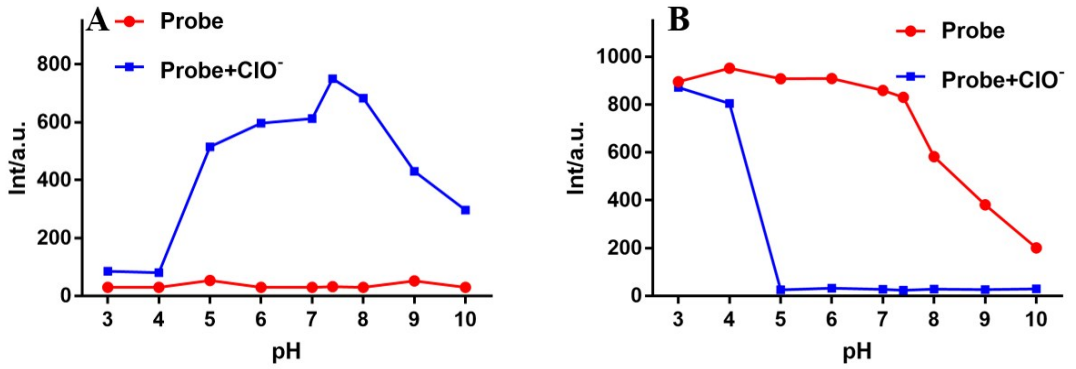

Fig. S8. The fluorescence emission intensity (A) (500 nm) and (B) (650 nm) of probe **2** (10 μM) under different pH (3-10) of in the absence and presence of ClO^- (100 μM). λ_{ex} = 566 nm, slits: 5.0/5.0 nm at 650 nm; λ_{ex} = 420 nm, slits: 5.0/5.0 nm at 500 nm.

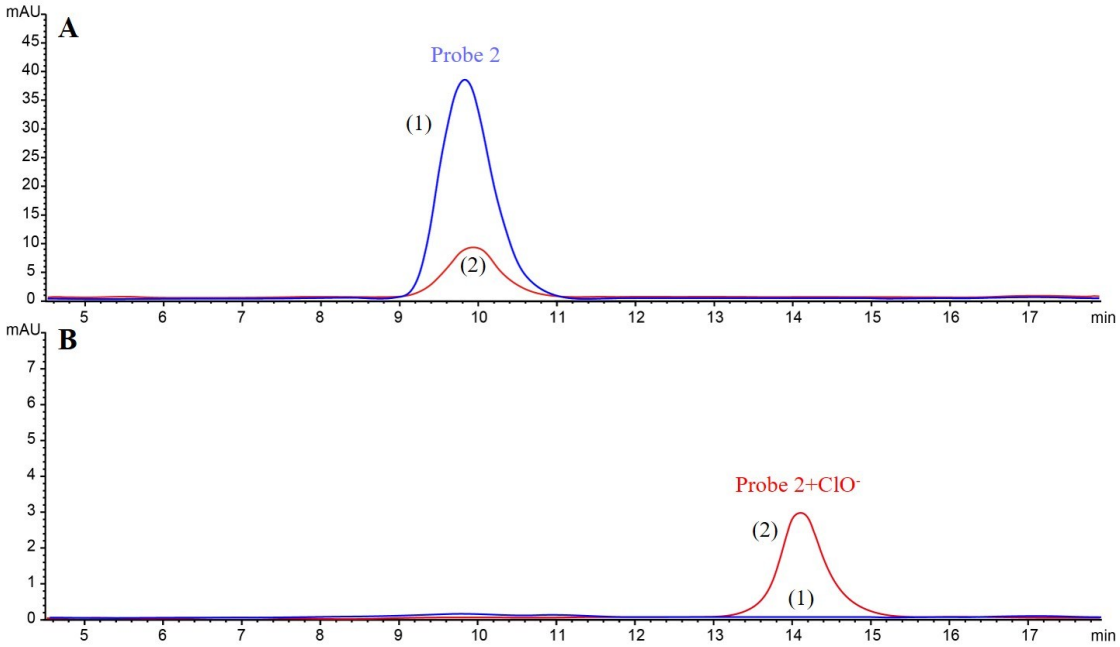

Fig. S9. HPLC chromatogram in the reaction of ClO^- to probe **2**. (A) Probe **2** (100 μM) in PBS (pH 7.4) buffer at peak (1) and probe **2** (100 μM) reacted with ClO^- (3 equiv.) for 2 min at peak (2). Method: Reversed-phase column were selected as the chromatographic conditions with methanol: 0.1% formic acid water solution (v/v = 95: 5) as the mobile phase, on the basis of 1.0 mL/min at 560 nm wavelength, at 30 °C column temperature to complete the correlation detection for the sample; (B) No peak (1) for probe **2** and new products formed at peak (2) after the reaction of probe **2** (100 μM) with ClO^- (3 equiv.) for 2 min. Method: Reversed-phase column were selected as

the chromatographic conditions with methanol: 0.1% formic acid water solution (v/v = 97: 3) as the mobile phase, on the basis of 1.0 mL/min at 400 nm wavelength, at 30 °C column temperature to complete the correlation detection for the sample.

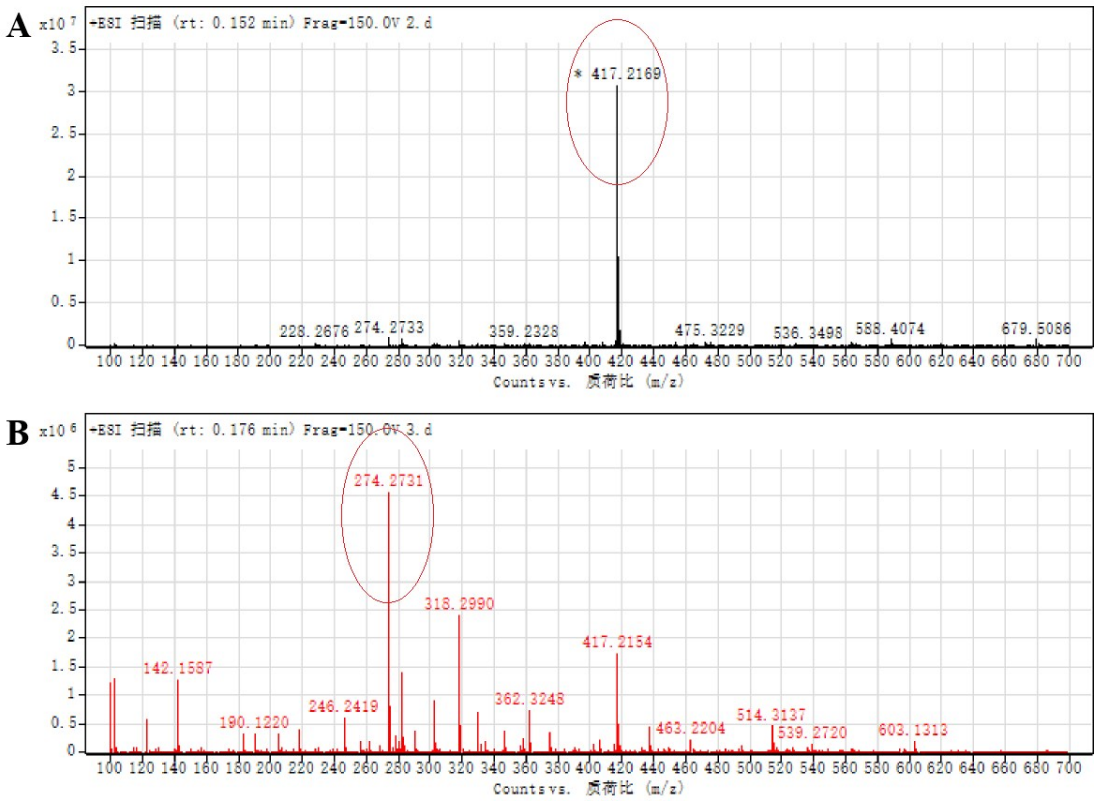

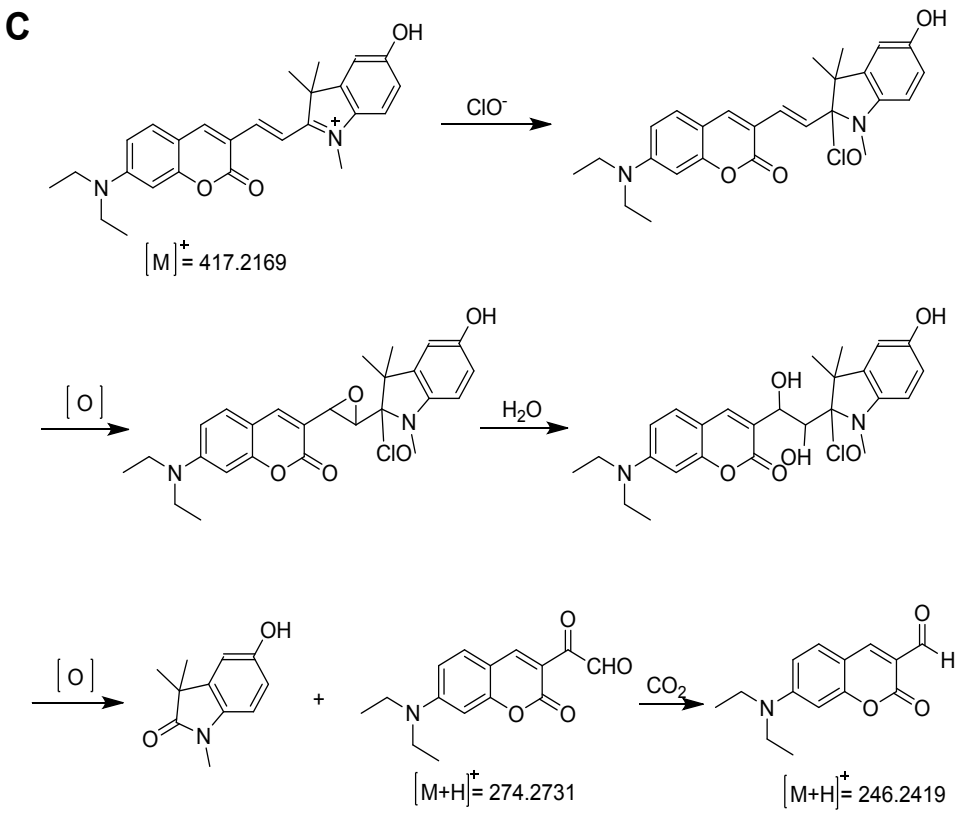

Fig. S10. Mass spectrum of probe **2** (A) and the crude product from the reaction of probe **2** with ClO^- (B); (C) Propose sensing mechanism of the probes for ClO^- by HR-MS.

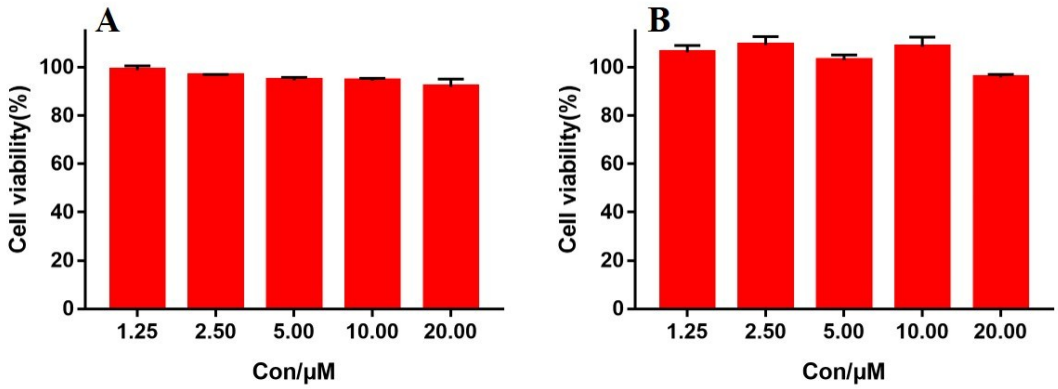

Fig. S11. CCK8 assay of RAW cells (A) and HepG2 cells (B) incubated in a series of concentrations for the probe **2** (0–20 μM) at 37 °C for 12 h.

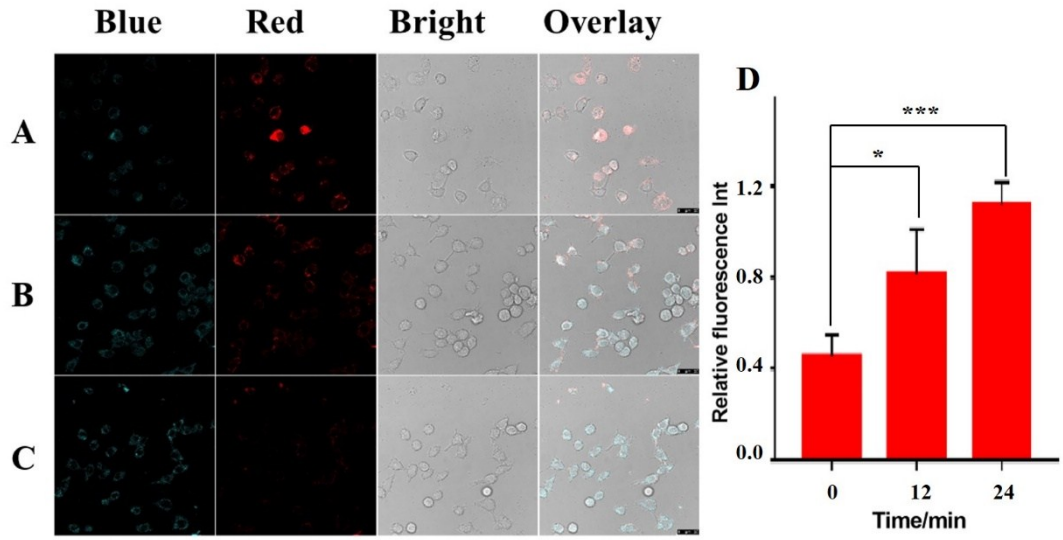

Fig. S12. Confocal fluorescence images of probe **2** (10 μM) for 1 h in RAW cells within the induction of LPS (2 μg/mL) under a set of time (A: 0 h, B: 12 h, C: 24 h). Quantification of imaging data for RAW cells (D): Relative mean fluorescence levels of cells were quantified by normalized intensity at blue channel (480-520 nm) and red channel (630-680 nm). Values are the mean ± SD for each group of three experiments; $*p < 0.05$, $***p < 0.001$.

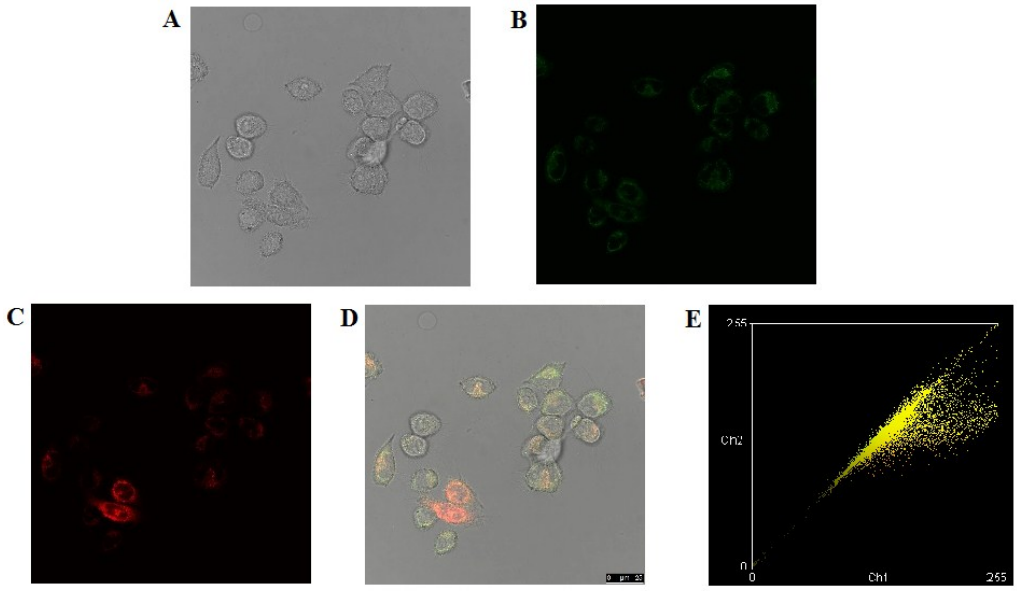

Fig. S13. Imaging of HepG2 cells stained with probe **2** (10 μM) for 2 h, Mito-Tracker Green FM (200 nM) for 2 h at 37 °C and then washed with PBS before imaging. (A): bright field image; (B): green channel image (from MitoTracker Green FM); (C): red

channel image (from probe **2**); (D): merged images of green channel and red channel; (E): Correlation plot of MitoTracker Green FM and probe intensities. Green channel: λ_{ex}= 488 nm; λ_{em} = 500-540 nm; Red channel: λ_{ex} = 552 nm; λ_{em} = 600-660 nm.

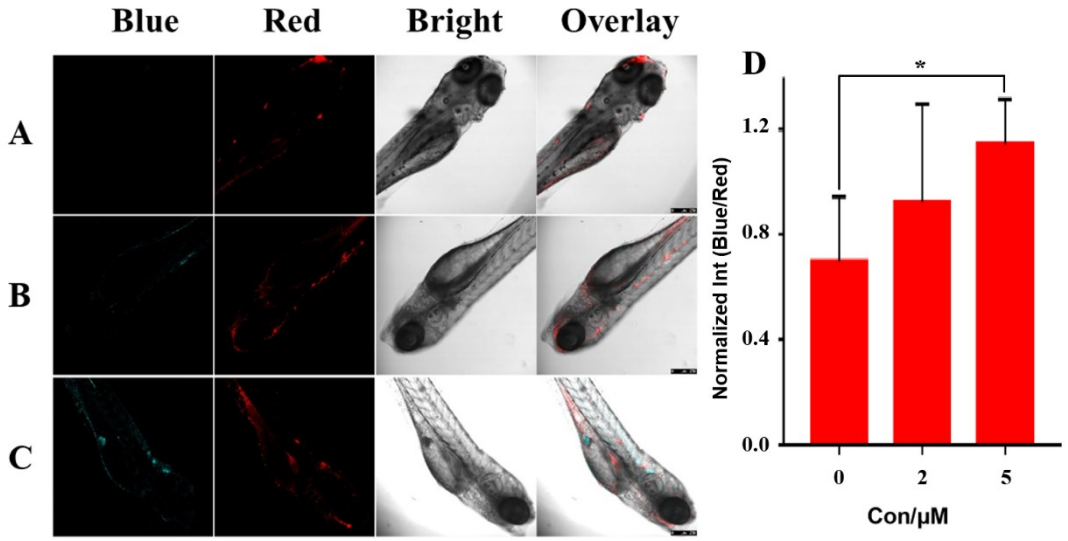

Fig. S14. Confocal fluorescence images of zebrafish incubated with probe **2** (10 μM) for 1 h and then treated with ClO^- at different concentrations (A: 0 μM, B: 2 μM, C: 5 μM) for 1 h; Quantification of imaging data for the addition of ClO^- (D): Relative mean fluorescence levels of cells were quantified by normalized intensity at blue channel (480-520 nm) and red channel (630-680 nm). Values are the mean ± SD for each group of three experiments; *p < 0.05.

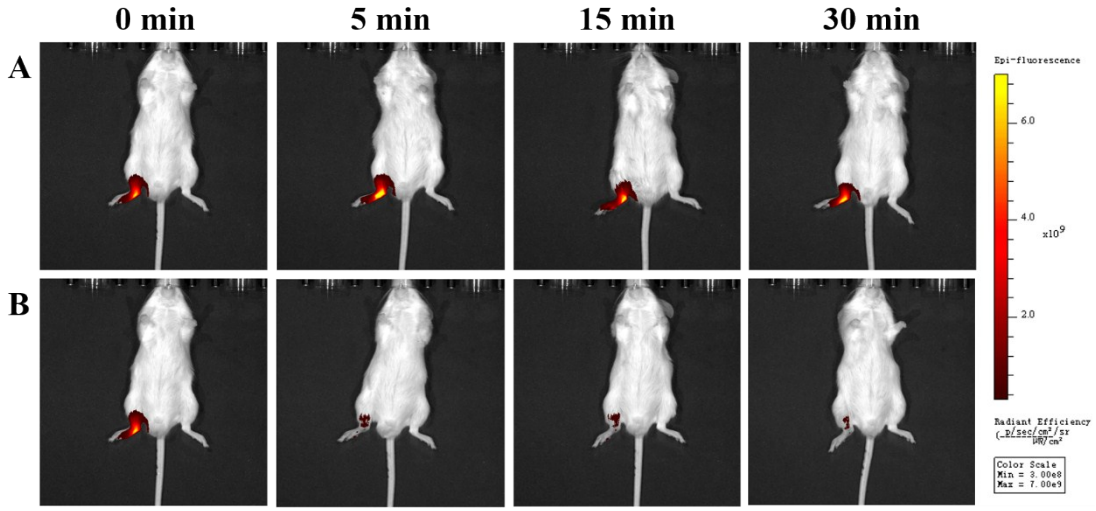

Fig. S15. Fluorescent images of mice injected with probe **2** (1 mM, 10 μL) for 10 min

and then treated with ClO^- at different concentrations (A: 0 μM, B: 200 μM; 10 μL) for 5 min, 15 min, 30 min; Red channel (λ_{ex} = 605 nm; λ_{em} = 650 nm).

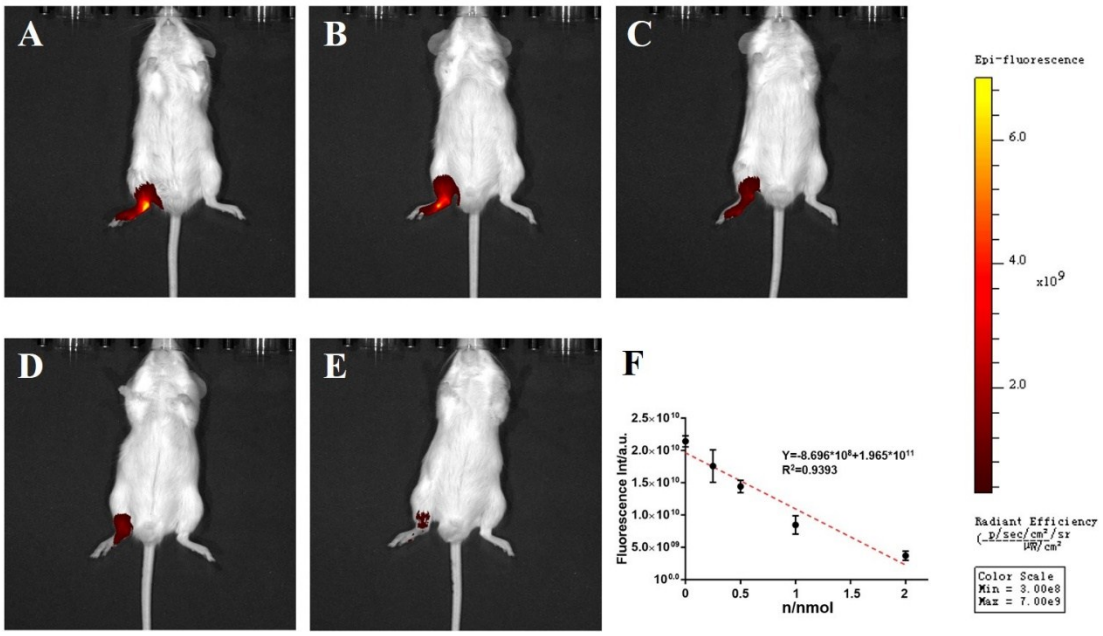

Fig. S16. Fluorescent images of mice injected with probe **2** (1 mM, 10 μL) for 10 min and then treated with ClO^- at different concentrations (A: 0 nmol, B: 0.25 nmol, C: 0.5 nmol, D: 1 nmol, E: 2 nmol) for 5 min; Quantification of imaging data for the addition of ClO^- (F): Relative mean fluorescence levels of ankles were quantified by normalized intensity at red channel (λ_{ex} = 605 nm; λ_{em} = 650 nm.).

Supplemental references

S1. X. Zhou, Y. Kwon, G. Kim, J.-H. Ryu and J. Yoon, *Biosensors & Bioelectronics*, 2015, **64**, 285-291.

S2. J.-T. Hou, H. S. Kim, C. Duan, M. S. Ji, S. Wang, L. Zeng, W. X. Ren and J. S. Kim, *Chemical Communications*, 2019, **55**, 2533-2536.

S3. Y.-H. Yan, H.-L. Ma, J.-Y. Miao, B.-X. Zhao and Z.-M. Lin, *Analytica Chimica Acta*, 2019, **1064**, 87-93.

S4. K. Zhang, Y. Lv, J. Meng, J. Wang, A. Peng, X. Wang and Z. Tian, *Analytica Chimica Acta*, 2019, **1061**, 142-151.

S5. J. Liu and Z. Yin, *Talanta*, 2019, **196**, 352-356.

S6. C. Duan, M. Won, P. Verwilst, J. Xu, H. S. Kim, L. Zeng and J. S. Kim, *Analytical Chemistry*, 2019, **91**, 4172-4178.

S7. Z. Wang, Y. Zhang, J. Song, Y. Yang, X. Xu, M. Li, H. Xu and S. Wang, *Analytica Chimica Acta*, 2019, **1051**, 169-178.

S8. X. Xie, T. Wu, X. Wang, Y. Li, K. Wang, Z. Zhao, X. Jiao and B. Tang, *Chemical Communications*, 2018, **54**, 11965-11968.

S9. M. Ren, Z. Li, J. Nie, L. Wang and W. Lin, *Chemical Communications*, 2018, **54**, 9238-9241.

S10. L. Wu, Q. Yang, L. Liu, A. C. Sedgwick, A. J. Cresswell, S. D. Bull, C. Huang and T. D. James, *Chemical Communications*, 2018, **54**, 8522-8525.

S11. C. Zhang, Q. Nie, I. Ismail, Z. Xi and L. Yi, *Chemical Communications*, 2018, **54**, 3835-3838.